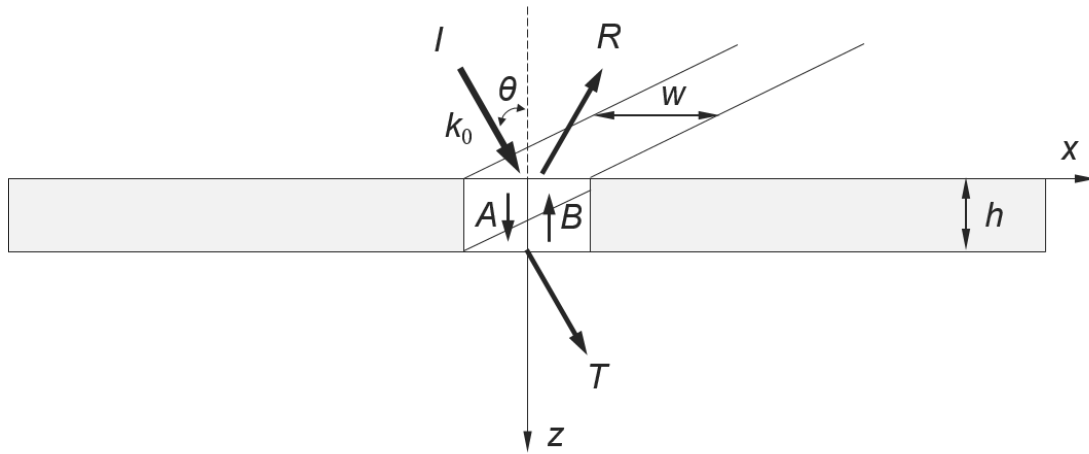


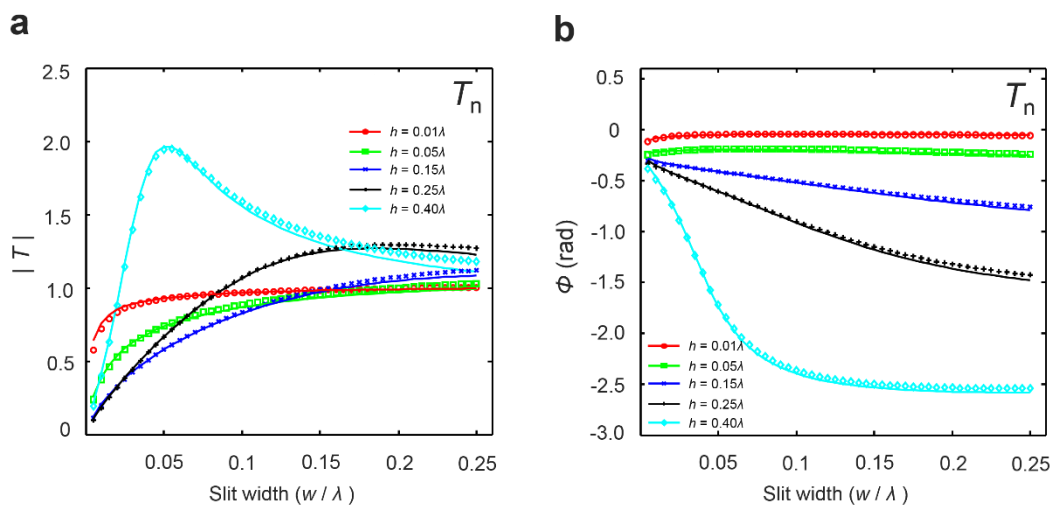
Supplementary Information

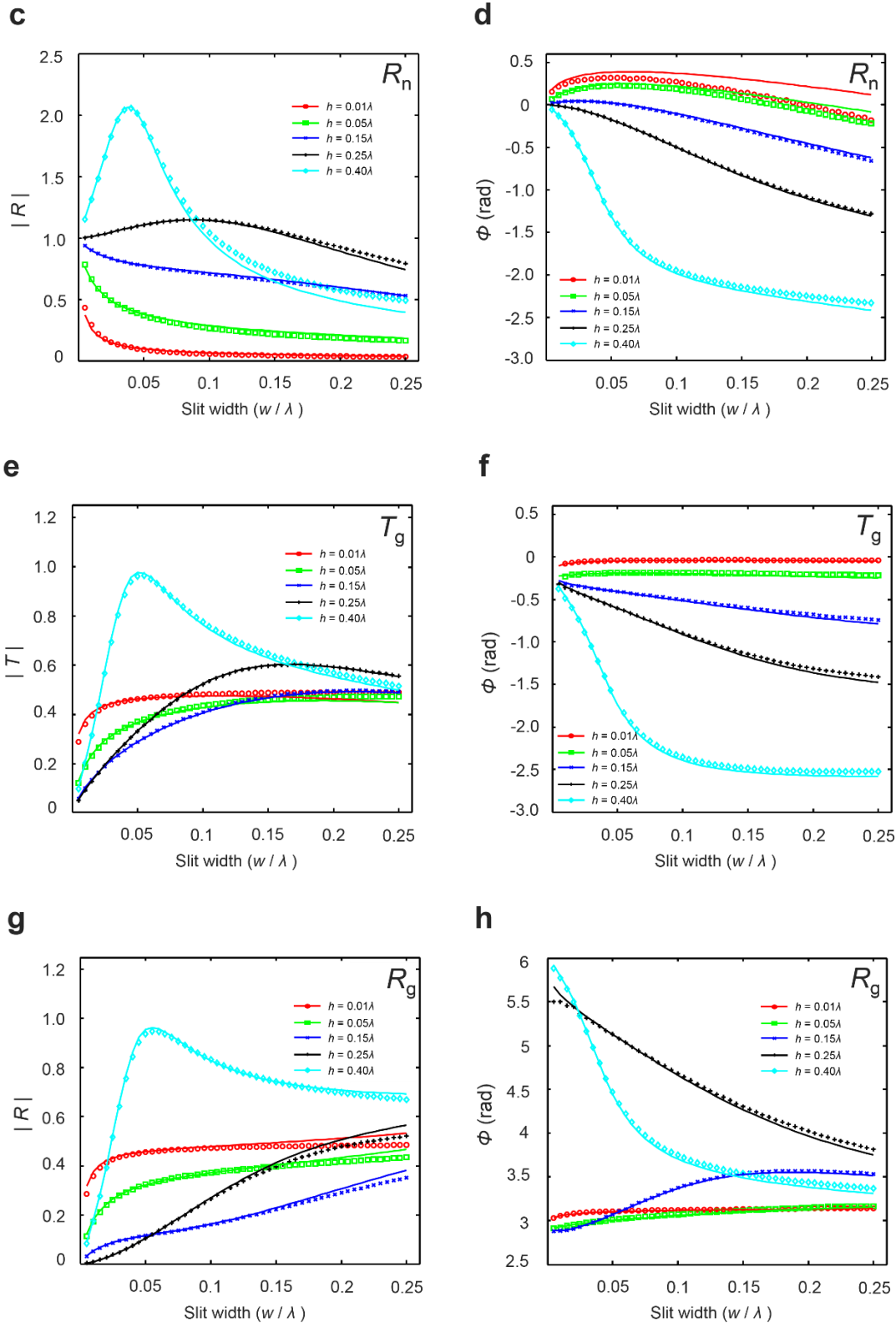
Deep-subwavelength control of acoustic waves in an ultra-compact metasurface lens

Chen et al.

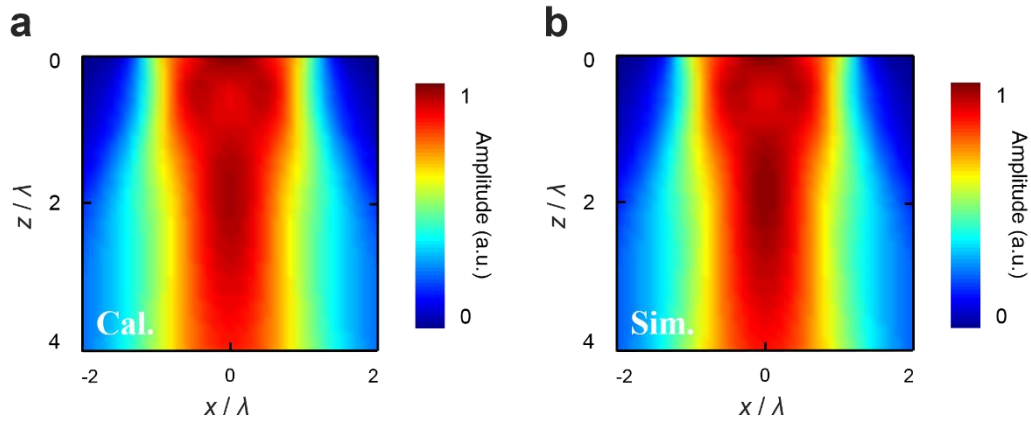


Supplementary Figure 1 | Schematic diagram of wave interactions with a subwavelength slit. The slit has a rectangular cross-section with width w and thickness h . The pressure field of incident waves is normalized to 1 Pa.

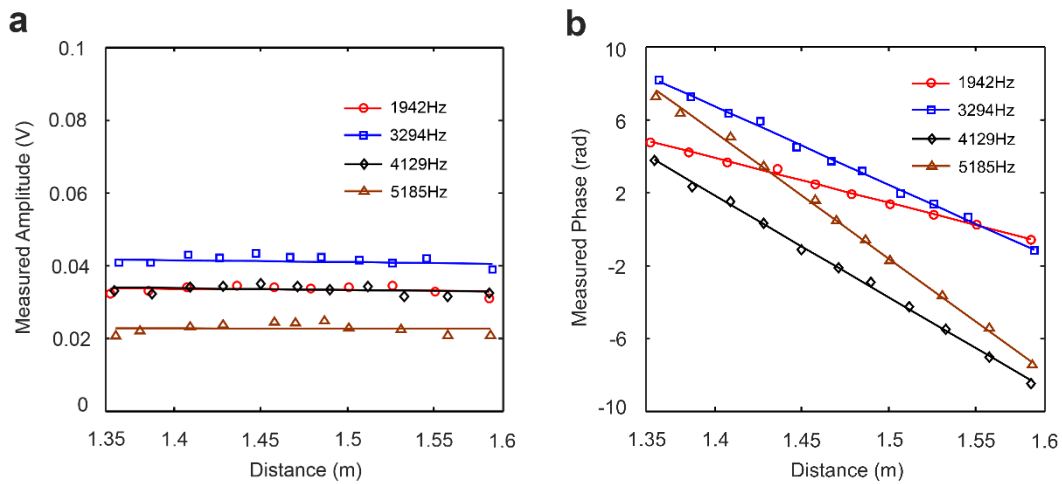




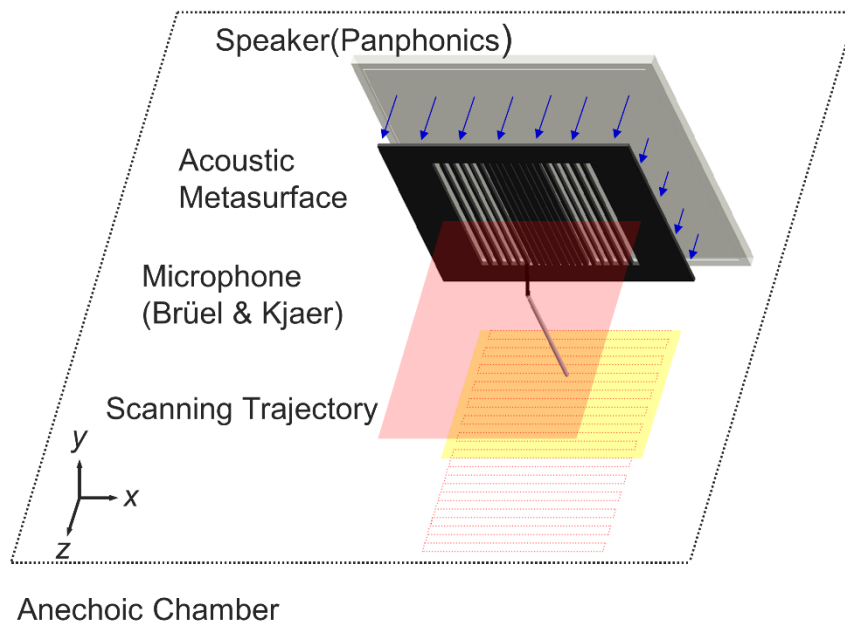
Supplementary Figure 2 | The comparisons of transmission and reflection coefficients of a single slit between theoretical calculations (solid lines) and numerical simulations (marks). The calculation and simulation for (a, b) T_n , (c, d) R_n , (e, f) T_g and (g, h) R_g are carried out on different slit parameters. The slit width increases from 0.005λ to 0.25λ with a step of 0.005λ at different thicknesses ($h = 0.01\lambda, 0.05\lambda, 0.15\lambda, 0.25\lambda, 0.4\lambda$).



Supplementary Figure 3 | (a) Calculated and (b) simulated pressure field after a plane wave transmits through a user-defined acoustic metasurface. The thickness, spacing, and slit number in the acoustic metasurface are 0.1λ , 0.15λ and 19, respectively. The slit widths decrease from 0.1λ to 0.01λ with a step of 0.01λ from the center to the side.



Supplementary Figure 4 | (a) The amplitude and (b) phase of the acoustic signals generated by the plane wave speaker at selected frequencies: 1942Hz (circles), 3294Hz (squares), 4129Hz (diamonds) and 5185Hz (triangles). The measurements were performed along the 45° diagonal path in front of the speaker on which the microphone slides. The distance of the measurement locations was recorded with respect to a reference point on the frame diagonal. The measured phase data was fitted using linear least squares, and the parameters are listed in Supplementary table 3.



Supplementary Figure 5 | Schematic of the experimental setup for acoustic field measurements.

m	1	2	3	4	5	6	7	8	9	10
slit width (0.01λ)	14.1	12.3	12.6	12.6	11.9	7.0	3.0	2.0	2.0	2.1
m	11	12	13	14	15	16	17	18	19	
slit width (0.01λ)	2.0	2.0	3.0	7.0	11.9	12.6	12.6	12.3	14.1	

Supplementary Table 1: Optimized slit widths of the acoustic metasurface lens for far-field sound focusing.

m	1	2	3	4	5	6	7	8	9	10	11
slit width (0.01λ)	0.3	0.32	0.34	5.32	1.58	8.94	1.58	5.32	0.34	0.32	0.3

Supplementary Table 2: Optimized slit widths of the near-field metasurface lens.

Frequency (Hz)	Theoretical phase slope (rad m ⁻¹)	Experimental phase slope (rad m ⁻¹)	R^2 value
1942	-25.15	-24.47	0.9954
3294	-42.67	-43.13	0.9981
4129	-53.48	-56.02	0.9986
5185	-67.16	-67.06	0.9969

Supplementary Table 3: The linear least square fitting parameters of the measured phases.

Supplementary Note 1. The Derivation of transmission and reflection coefficients

Consider an amplitude-normalized plane wave with a tangential component of wave-vector α_0 incident on a rigid plate, as shown in Supplementary Fig. 1. The slit has a rectangular cross-section with width w and thickness h . Under this insonification, the expression of the pressure field above and below the slit can be, respectively, written as

$$P_a = P_t + P_r = e^{i\alpha_0 x + i\eta_0 z} + \int_{-\infty}^{+\infty} R(\alpha) e^{i\alpha x - i\eta z} d\alpha \quad (\text{A.1})$$

and

$$P_b = P_t = \int_{-\infty}^{+\infty} T(\alpha) e^{i\alpha x + i\eta(z-h)} d\alpha, \quad (\text{A.2})$$

where $i = \sqrt{-1}$, $\eta_0 = \sqrt{k_0^2 - \alpha_0^2}$ is the z component of the incident-wave vector, α and $\eta = \sqrt{k_0^2 - \alpha^2}$ are the wave vectors of high-order diffraction along x and z directions, respectively; $k_0 = \omega / c$ is the wave-vector of the incident wave in air (ω is the angular frequency and c is the acoustic velocity in air); $R(\alpha)$ and $T(\alpha)$ are the reflection and transmission coefficients, respectively. By making Fourier transforms of each waveguide modes, $R(\alpha)$ and $T(\alpha)$ can be expanded as¹

$$R(\alpha) = \delta(\alpha - \alpha_0) + \sum_{j \geq 0} R_j W_j(\alpha) / \eta \quad (\text{A.3})$$

$$T(\alpha) = \sum_{j \geq 0} T_j W_j(\alpha) / \eta, \quad (\text{A.4})$$

where δ is the Dirac delta function, and

$$W_j(\alpha) = \int_{-w/2}^{w/2} e^{-i\alpha x} \cos\left(\frac{j\pi}{w} x\right) dx. \quad (\text{A.5})$$

Inside the slit, the pressure field is also expanded in terms of the waveguide modes, which is expressed as

$$P_{\text{in}} = \sum_{j \geq 0} \cos\left(\frac{j\pi}{w} x\right) [A_j e^{i\sqrt{k_0^2 - (\frac{j\pi}{w})^2} z} + B_j e^{-i\sqrt{k_0^2 - (\frac{j\pi}{w})^2} z}] \quad (\text{A.6})$$

where A_j and B_j are the pressure amplitudes of the forward and backward waves of j -th waveguide mode, and j is a positive integer.

In the case of a subwavelength slit, the pressure field can be sufficiently well described by the first term in the mode expansions (this means that only the fundamental mode ($j = 0$) is retained)¹. Therefore, Supplementary equations 1-6 can be simplified to

$$\begin{cases} P_a = e^{i\alpha_0 x + i\eta_0 z} + e^{i\alpha_0 x - i\eta_0 z} + \int_{-\infty}^{+\infty} \frac{R_0 W_0(\alpha)}{\eta} e^{i\alpha x - i\eta z} d\alpha \\ P_{in} = A_0 e^{ik_0 z} + B_0 e^{-ik_0 z} \\ P_b = \int_{-\infty}^{+\infty} \frac{T_0 W_0(\alpha)}{\eta} e^{i\alpha x + i\eta(z-h)} d\alpha \end{cases} \quad (\text{A.7-1})$$

with $W_0(\alpha) = \int_{-w/2}^{w/2} e^{-i\alpha x} dx = \frac{2 \sin(w\alpha/2)}{\alpha}$.

The normal velocities can then be obtained from $u = \frac{1}{i\rho\omega} \frac{\partial p}{\partial z}$, and thus we have

$$\begin{cases} u_a = \frac{1}{\rho\omega} (\eta_0 e^{i\alpha_0 x + i\eta_0 z} - \eta_0 e^{i\alpha_0 x - i\eta_0 z} - \int_{-\infty}^{+\infty} R_0 W_0(\alpha) e^{i\alpha x - i\eta z} d\alpha) \\ u_{in} = \frac{k_0}{\rho\omega} (A_0 e^{ik_0 z} - B_0 e^{-ik_0 z}) \\ u_b = \frac{1}{\rho\omega} \left(\int_{-\infty}^{+\infty} T_0 W_0(\alpha) e^{i\alpha x + i\eta(z-h)} d\alpha \right) \end{cases} \quad (\text{A.7-2})$$

where ρ is the mass density of air. According to the boundary conditions, the pressure field and normal velocity at the interfaces (i.e., $z = 0$ and $z = h$) should be continuous. Combining the continuity conditions with Supplementary equation 7, we can determine the coefficients R_0 , T_0 , A_0 , and B_0 .

Firstly, we calculate the transmission and reflection coefficients [T_n and R_n] for a normally incident plane wave. Under the normal incidence ($\theta = 0$), we have $\alpha_0 (=k_0 \sin\theta) = 0$ and $\eta_0 = k_0$. By substituting the initial conditions to Supplementary equation 7 and applying the boundary conditions at $z = 0$, we obtain

$$\begin{cases} 2 + \int_{-\infty}^{+\infty} \frac{R_0 W_0(\alpha)}{\eta} e^{i\alpha x} d\alpha = A_0 + B_0 \\ \int_{-\infty}^{+\infty} R_0 W_0(\alpha) e^{i\alpha x} d\alpha = -k_0 (A_0 - B_0) \end{cases} \quad (\text{A.8-1})$$

Similarly, at $z = h$

$$\begin{cases} \int_{-\infty}^{+\infty} \frac{T_0 W_0(\alpha)}{\eta} e^{i\alpha x} d\alpha = A_0 e^{ik_0 h} + B_0 e^{-ik_0 h} \\ \int_{-\infty}^{+\infty} T_0 W_0(\alpha) e^{i\alpha x} d\alpha = k_0 (A_0 e^{ik_0 h} - B_0 e^{-ik_0 h}) \end{cases} \quad (\text{A.8-2})$$

Note that although the slits are deep-subwavelength compared to the incident wave, they cannot be simply considered as points for all waves, especially the evanescent waves with large tangential wave-vectors. As the integration is performed for all wave components over $[-\infty, \infty]$, here we generalize the evaluation of $e^{i\alpha x}$ by averaging it on the whole slit width, to integrate out the x

dependence. Thus, we have $e^{i\alpha x} \approx \frac{1}{w} \int_{-w/2}^{w/2} e^{i\alpha x} dx = \frac{2 \sin(w\alpha/2)}{\alpha w}$. Substituting $e^{i\alpha x}$ and

$W_0(\alpha) = \frac{2 \sin(w\alpha/2)}{\alpha}$ into Supplementary equation 8, we therefore have

$$\begin{cases} T_n = \int_{-\infty}^{\infty} \frac{T_0 W_0(\alpha)}{\eta} e^{i\alpha x} d\alpha = \frac{4Qe^{ik_0 h}}{(Q+1)^2 - (Q-1)^2 e^{2ik_0 h}} \\ R_n = 1 + \int_{-\infty}^{\infty} \frac{R_0 W_0(\alpha)}{\eta} e^{i\alpha x} d\alpha = \frac{Q-1}{Q+1} (T_n e^{ik_0 h} - 1) \end{cases} \quad (\text{A.9})$$

with $Q = \frac{k_0}{\pi w} \int_{-\infty}^{\infty} \frac{1 - \cos(w\alpha)}{\alpha^2 \sqrt{k_0^2 - \alpha^2}} d\alpha$.

Similar calculations are implemented to the grazing incidence by changing the initial conditions to $\alpha_0 = k_0$ and $\eta_0 = 0$, and finally we get

$$\begin{cases} T_g = \frac{2Qe^{ik_0 h} \text{sinc}(k_0 w/2)}{(Q+1)^2 - (Q-1)^2 e^{2ik_0 h}} \\ R_g = \frac{T_g e^{ik_0 h} (Q-1) + \text{sinc}(k_0 w/2)}{Q+1} - 1 \end{cases} \quad (\text{A.10})$$

Supplementary Note 2. Characteristic parameters of the cylindrical waves (CWs)

Under uniform illumination by a (normal or grazing) plane wave, the acoustic wave scattered by a subwavelength slit can be regarded as a new point source that thus generates a CW. The excited CW can be characterized by two coefficients, β and ϕ . To extract the coefficients, a two-step procedure is adopted. Firstly, the pressure field is extracted through a numerical simulation. Then, using Eq. (1) in the main text, the coefficients are optimized by fitting the pressure field distribution over an interval ($w/2 \leq r \leq 10\lambda$). This procedure offers a rigorous numerical approach to calculate β and ϕ , and similar calculations are performed for different slit parameters. The slit width increases from 0.005λ to 0.2λ with a step of 0.005λ at different thicknesses ($h = 0.05\lambda, 0.1\lambda, 0.3\lambda, 0.7\lambda, 0.9\lambda$). The calculated β and ϕ for different slits are provided in the Source Data file. From these calculations, it can be found that both β and ϕ are relying on the slit width w , but independent of thickness h . To determine the relationship between the CWs and the slit parameters, β and ϕ are fitted as a polynomial function of slit width with the least-mean-square method.

Supplementary References

1. Takakura, Y. Optical resonance in a narrow slit in a thick metallic screen. *Phys. Rev. Lett.* 86, 5601 (2001).